Journal of Adult Congenital Heart Disease Vol.4 No.2(2015) 69-73

【Original Article】

Clinical Impact of Interventricular Dyssynchrony in Repaired Tetralogy of Fallot: Myocardial Strain Analysis Using Semi-automatic Tracking of Cine Magnetic Resonance Imaging

Masateru Kawakubo, PhD[1)], Yuzo Yamasaki, MD[2)], Ichiro Sakamoto, MD[3)], Kenichiro Yamamura, MD[4)], Michinobu Nagao, MD[5)]

[1)]Department of Radiological Technology, Faculty of Fukuoka Medical Technology, Teikyo University,
[2)]Department of Clinical Radiology, Graduate School of Medical Sciences, Kyushu University,
[3)]Department of Cardiovascular medicine, Graduate School of Medical Sciences, Kyushu University,
[4)]Department of Pediatrics, Graduate School of Medical Sciences, Kyushu University,
[5)]Department of Molecular Imaging & Diagnosis, Graduate School of Medical Sciences, Kyushu University

Abstract

Background: The interventricular dyssynchrony (IVD) is one of important functional parameters for patients with adult congenital heart disease (ACHD). In this study, we proposed semi-automatic myocardial strain analysis using 4-chamber (4CH) cine magnetic resonance imaging (MRI) to calculate IVD, and investigated the clinical impact of IVD in patients with repaired tetralogy of Fallot (TOF).

Methods: Data of cardiac MRI with 3-Teslar in 30 patients with repaired TOF was retrospectively analyzed. The longitudinal strains of biventricular free walls in the 4CH cine MRI were calculated using semi-automatic strain analysis. IVD was defined as a delay duration between peak times of longitudinal strain for right and left ventricles. Pulmonary regurgitant fraction (PRF, %) was derived from phase-contrast MRI. Comparison of IVD between repaired TOF patients with PRF of <30% and >30% was analyzed by Wilcoxon rank-sum test. Receiver-operating-characteristic (ROC) analysis was performed to determine the optimal cutoff of IVD for differentiating patients with PRF >30%.

Results: IVD was significantly greater for patients with PRF >30% than those with PRF <30% (63.7 ± 31.0 ms vs. 32.4 ± 23.2 ms, $p = 0.004$). ROC analysis revealed optimal cutoff IVD of 45.8 ms for differentiating patients with PRF >30% from patients with PRF <30% with C-statistics of 0.83, a sensitivity of 86%, and a specificity 70 %.

Conclusions: IVD obtained from semi-automatic myocardial strain analysis of cine MR imaging is related to the severity of pulmonary regurgitation in repaired TOF, and has a clinical impact on determination of the treatment strategy.

Key words：repaired tetralogy of Fallot, cardiac magnetic resonance imaging, interventricular dyssynchrony, myocardial strain

Introduction

Improvement of surgical care for congenital heart disease leads to a growing number of patients with adult congenital heart disease (ACHD) [1-3)]. Patients with ACHD often have interventricular dyssynchrony (IVD) due to right ventricular (RV) volume or pressure overload [4,5)]. Although the impact of left ventricular (LV) dyssynchrony in ACHD patients has already been investigated [6-8)], the impact of IVD has not been fully investigated.

We previously reported that longitudinal strain analysis using 4-chamber (4CH) cine magnetic resonance imaging (MRI) could predict the response to cardiac resynchronization therapy in advanced heart failure [9)]. This method evaluates

Corresponding author: Michinobu Nagao, MD
Department of Molecular Imaging & Diagnosis, Graduate School of Medical Sciences, Kyushu University
3-1-1 Maidashi, Higashi-Ku Fukuoka-city Fukuoka 812-8582, Japan
Phone: +81-92-642-5695 Fax: +81-92-642-5708 E-mail: minagao@radiol.med.kyushu-u.ac.jp

cardiac dyssynchrony by manual measurement of the lengths of the LV and RV free wall through a cardiac cycle. In another study, an MRI feature tracking technique that can extract cardiac contours semi-automatically and accurately [10,11] is applied for longitudinal strain analysis using 4CH cine MRI [12]. The purpose of this study is to quantify IVD using this new semi-automatic method and to investigate the clinical impact of IVD in patients with repaired tetralogy of Fallot (TOF).

Materials and Methods

Patients

The study protocol was reviewed and approved by the institutional review board, and written informed consent was obtained from all patients.

Thirty consecutive patients with repaired TOF who underwent cardiac MRI were retrospectively enrolled between January and December 2014. In addition, 5 patients who had normal cardiac function and no prior cardiac disease were enrolled as controls. All patients had sinus rhythm on electrocardiography (ECG). Table 1 shows clinical characteristics and ventricular function.

Table 1 Patients Characteristics

	Repaired TOF (n = 30)	Control (n = 5)
Clinical characteristics		
Age	30 ± 12	65 ± 5
Female	14	3
Heart rate (beat / min)	69 ± 12	59 ± 7
QRS duration (ms)	131 ± 35	87 ± 9
CMR measurements		
LV function		
EDV (ml)	136 ± 38	122 ± 21
ESV (ml)	64 ± 19	47 ± 18
EF (%)	52 ± 6	63 ± 10
RV function		
EDV (ml)	217 ± 86	
ESV (ml)	126 ± 71	
EF (%)	44 ± 9	

Baseline characteristics of all patients are shown.
CMR: cardiac magnetic resonance, LV: left ventricular, RV: right ventricular, EDV: end diastole volume, ESV: end systolic volume, EF: ejection fraction

MRI protocol

All MRI examinations were performed in a supine position using a 3.0T system (Achieva 3.0T TX; Philips Medical Systems, Best, the Netherlands) with a 32-element cardiac coil using ECG gating. The 4CH cine images of 20 cardiac phases / RR intervals on the ECG were obtained by steady state free precession (SSFP) sequences. The imaging protocol was as follows: TR = 2.9 ms, TE = 1.5 ms, flip angle = 45°, slice thickness = 8 mm, field of view 380 mm × 380 mm, acquisition matrix = 176 × 162, and reconstruction matrix = 512 × 512. Phase contrast (PC) MRI with a flow-sensitive gradient echo sequence was obtained for 30 cardiac phases. The imaging protocol was as follows: TR = 6.5 ms, TE = 4.0 ms, flip angle = 10°, slice thickness = 3 mm, field of view 320 mm × 300 mm, acquisition matrix = 128 × 256, and velocity encoded value (VENC) set to 100 - 250 cm / s.

Cine images were analyzed using commercial software (Extended Work space, Philips Healthcare, Best, The Netherlands). The LV and RV volumes were measured at end-diastole and end-systole by manually tracing endocardial contours from base to apex on the short-axis cine MRI. The LV ejection fraction (LVEF) was calculated from LV end-diastolic and systolic volumes. The RV ejection fraction (RVEF) was similarly obtained with transverse cine MRI.

In patients with repaired TOF, the pulmonary regurgitant fraction (PRF, %) was defined as the percentage of the retrograde to anterograde flow for the main pulmonary artery, and was calculated from time-flow curves derived from phase-contrast MRI (Fig. 1).

Semi-automatic myocardial strain analysis

LV and RV free walls were semi-automatically delineated as a polygonal line with control points. First, the LV and RV free walls were manually delineated on the 4CH MRI only at end-diastole (Fig. 2a). Second, the control points were automatically set on the delineated line on the ventricular free wall at each interval of 25 pixels (Fig. 2b). Third, control points were propagated for a cardiac cycle with a local template matching technique similar to the MRI feature tracking technique (Fig. 2c). The square template size and square search area were configured for 25 × 25

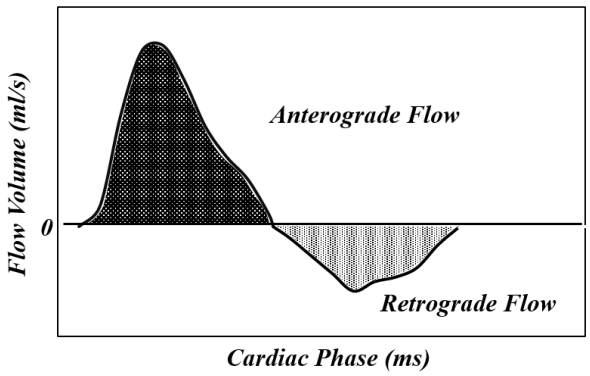

Fig. 1 Pulmonary regurgitant fraction in repaired TOF

Pulmonary regurgitant fraction (PRF, %) was calculated from PC MRI as the percentage of the retrograde flow volume to anterograde flow volume for main pulmonary artery.

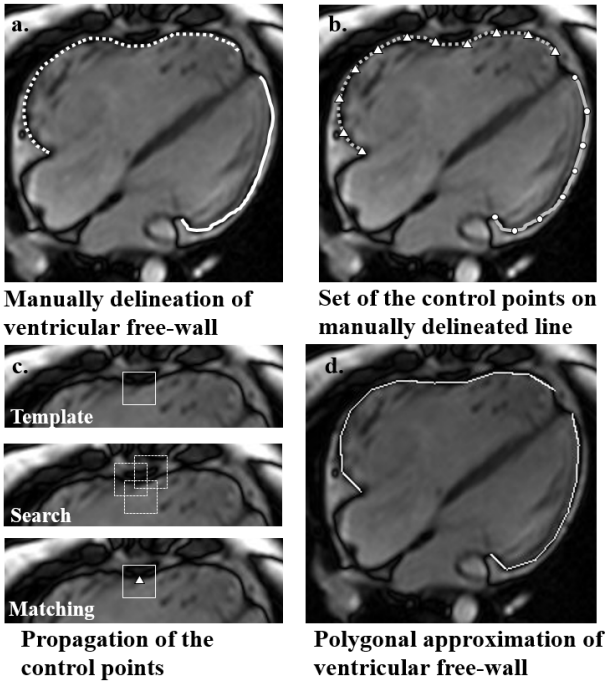

Fig. 2 Semi-automatic myocardial strain analysis

a. First-step, ventricular free walls were manually delineated (LV: solid line, RV: dashed line) only at the end-diastole 4CH MRI.
b. Second-step, the control points were automatically set on the delineated line on ventricular free wall at each interval of 25 pixels.
c. Third-step, control points were propagated for a cardiac cycle with the local template matching technique (upper to lower). The square template size and square search area were configured for 25 × 25 pixels in size.
d. Final-step, the longitudinal lengths of ventricular free walls were calculated as the summation of the distances of the each point throughout cardiac cycle.

pixels in size for all tracking. Finally, the longitudinal lengths of the ventricular free walls were calculated as the summation of the distances of each point throughout a cardiac cycle (Fig. 2d).

The longitudinal strain was calculated as the percentage of the differences between the longitudinal length at each phase and end-diastole to the longitudinal length at end-diastole. The IVD (ms) was defined as the time delay between the peak times of longitudinal strain for LV to RV (Fig. 3).

Statistics

Continuous data are expressed as the means ± standard deviation (SD). Comparison of IVD between the two groups was analyzed by the Wilcoxon rank-sum test. Receiver-operating-characteristics (ROC) analysis was performed the optimal cutoff parameters for predicting repaired TOF patients with PRF of >30%. Correlations between IVD and right ventricular end-diastolic volume (RVEDV), and between IVD and QRS duration were analyzed using Pearson correlation coefficients in patients with repaired TOF, respectively. All statistical analyses were performed using SAS software for Windows (version 11, SAS Inc., Cary, NC, USA). All statistical tests were two-sided. A p value of < 0.05 was considered significant.

Results

IVD was significantly greater for patients with repaired TOF than controls (45.5 ± 31.6 ms vs. 9.4 ± 21.0 ms, $p = 0.02$).

In patients with repaired TOF, PRF could not be calculated in 3 patients due to metallic artifact and post-operative changes. PRF for 27 patients was 32.6 ± 24.3 %. IVD was significantly greater for patients with PRF >30% (n = 13) than patients with PRF <30% (n = 14) (63.7 ± 31.0 ms vs. 32.4 ± 23.2 ms, $p = 0.004$) (Fig. 4). ROC analysis revealed optimal cutoff IVD of 45.8 ms for differentiating patients with PRF >30% from patients with that <30% with C-statistics of 0.83, a sensitivity of 86%, and a specificity 70 %. A significant correlation between IVD and RVEDV ($r = 0.47$, $p < 0.01$) were observed (Fig. 5). No significant correlation between the IVD and QRS duration was observed ($r = 0.20$).

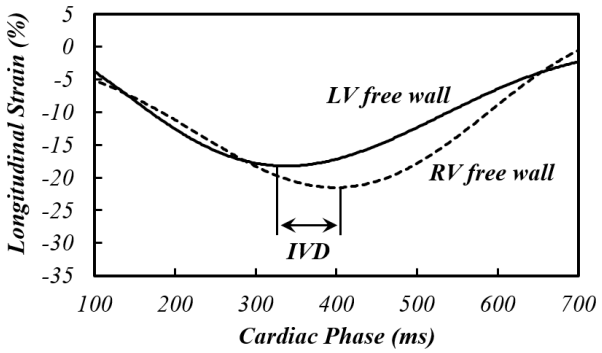

Fig. 3 Calculation of IVD

IVD was defined as a delay time between end-systolic times for biventricular free-walls.

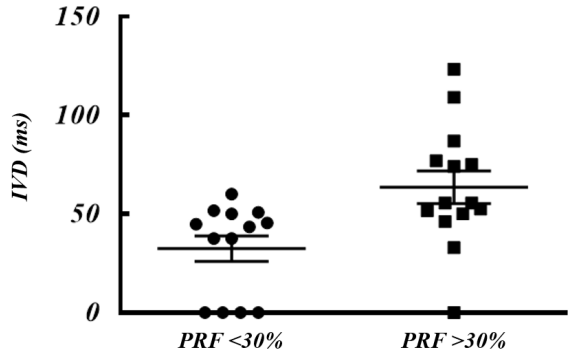

Fig. 4 Comparison of IVD between the patients with and without pulmonary regurgitation

IVD was significantly greater for patients with PRF >30% than those with PRF <30% (63.7 ± 31.0 ms vs. 32.4 ± 23.2 ms, p = 0.004).

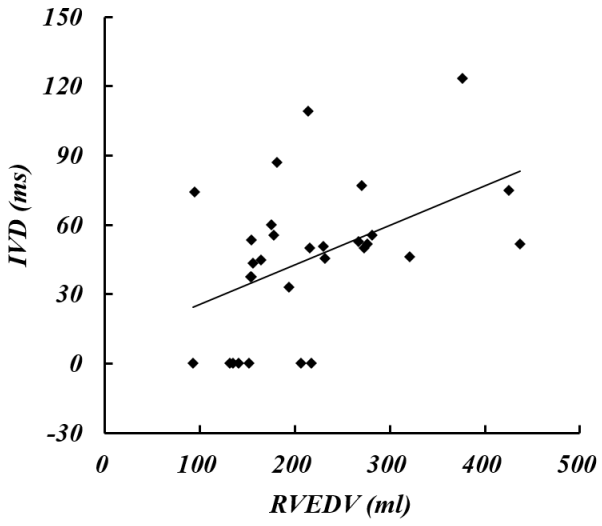

Fig. 5 Correlation between IVD and RVEDV

Significantly correlation between IVD and RVEDV was observed (r = 0.47, P < 0.01).

Discussion

The present study proposed semi-automatic myocardial strain analysis of cine MRI to calculate IVD. In patients with repaired TOF, IVD was helpful for detecting of severe pulmonary regurgitation. PC MRI has a limitation in the calculations of PRF. Main pulmonary artery flow cannot be measured due to metallic artifact and post-operative changes in prior pulmonary valve replacement. Actually, PRF could not be measured in 3 patients with repaired TOF in this study. Tricuspid regurgitation (TR) caused by RV volume or pressure overload in repaired TOF might affect pulmonary artery flow. In the present study, both PRF and IVD tended to be greater in 5 patients with TR than those in 22 patients without TR (PRF; 41.8 ± 24.0 % vs. 30.5 ± 23.9 %, IVD; 65.5 ± 29.0 ms vs. 41.5 ± 30.5 ms). According to this result, IVD might be more progress in patients with TR than patients with only pulmonary regurgitation. IVD obtained from tagged MRI can detect the RV dysfunction in ACHD patients [4], and IVD obtained from echocardiography is significantly longer for repaired TOF patients than control [5]. Our results completely agreed with these previous reports. Therefore, IVD is a candidate to determine the treatment strategy in repaired TOF, and is a helpful tool in routine cardiac MRI protocols without a special scan such as tagging MRI. As indicated in the results, no association between QRS duration and IVD suggests that prolonged QRS is not equal to the presence of mechanical dyssynchrony. Despite a high incidence of complete or incomplete right bundle branch block in patients with repaired TOF, the interval from QRS onset to rapid RV pressure upstroke (i.e., RV systolic time interval) was not prolonged [13]. This is most probably the result of peripheral bundle branch block of the genesis of the QRS pattern by right ventricular hypertrophy. In ACHD, prolonged QRS complexes and RV apical site pacing tend to be associated with a greater risk of pacing-induced ventricular dysfunction [14]. This is caused by the fact that prolonged QRS is not equal to a delay in RV contraction. Accordingly, IVD might reflect more strictly a delay in RV contraction than QRS duration.

Tagged MRI has generally been used in

myocardial strain analysis [4,15]. However, tagged MR imaging has restrictions to appending tags to the RV because of the complex RV structure in ACHD. Our semi-automatic myocardial strain analysis is based on an algorithm with matching of the template image. Accordingly, our method is a simple and accurate method to quantify myocardial strain. This is a great advantage in the assessment of longitudinal RV function, compared with tagging MRI. Furthermore, this algorithm may possibly be applied to LV short axis or 2-chamber cine MRI. Additional strain parameters and geometric cardiac motion analysis are possible [16-19].

Limitation

Although our study was limited by small number of patients and controls, our proposed method can be applied in various ACHD conditions, such as ventricular septal defect and complete and corrected transposition of the great arteries, and can be validated for many patients in a future study.

Conclusion

In conclusion, IVD obtained from semi-automatic myocardial strain analysis of cine MR imaging is related to the severity of pulmonary regurgitation in repaired TOF, and has a clinical impact on determination of the treatment strategy.

Reference

1) Marelli AJ, Mackie AS, Ionescu-Ittu R et al. Congenital heart disease in the general population: changing prevalence and age distribution. Circulation. 2007; 115: 163-172.
2) Terai M, Niwa K, Nakazawa M et al. Mortality from congenital cardiovascular malformations in Japan, 1968 through 1997. Circ J 2002; 66: 484-488.
3) Perloff JK, Warnes CA. Congenital hearts disease in adults: a new cardiovascular specialty. Circulation 2001; 84: 1881-1890.
4) Nagao M, Yamasaki Y, Yonezawa M, et al. Interventricular Dyssynchrony Using Tagging MRI Predicts Right Ventricular Dysfunction in Adult Congenital Heart Disease. Congenit Heart Dis. 2015; 10: 271-280.
5) Mueller M, Rentzsch A, Hoetzer K et al. Assessment of interventricular and right-intraventricular dyssynchrony in patients with surgically repaired tetralogy of Fallot by two-dimensional speckle tracking. Eur J Echocardiogr. 2010; 11: 786-792.
6) Liang XC, Cheung EW, Wong SJ et al. Impact of right ventricular volume overload on three-dimensional global left ventricular mechanical dyssynchrony after surgical repair of tetralogy of Fallot. Am J Cardiol. 2008; 102: 1731-1736.
7) Raedle-Hurst TM, Mueller M, Rentzsch A et al. Assessment of left ventricular dyssynchrony and function using real-time 3-dimensional echocardiography in patients with congenital right heart disease. Am Heart J. 2009; 157: 791-798.
8) Ortega M, Triedman JK, Geva T et al. Relation of left ventricular dyssynchrony measured by cardiac magnetic resonance tissue tracking in repaired tetralogy of fallot to ventricular tachycardia and death. Am J Cardiol. 2011; 107: 1535-1540.
9) Kawakubo M, Nagao M, Kumazawa S et al. Evaluation of cardiac dyssynchrony with longitudinal strain analysis in 4-chamber cine MR imaging. Eur J Radiol. 2013; 82: 2212-2216.
10) Hor KN, Gottliebson WM, Carson C et al. Comparison of magnetic resonance feature tracking for strain calculation with harmonic phase imaging analysis. JACC Cardiovasc Imaging. 2010; 3: 144-151.
11) Kawakubo M, Nagao M, Kumazawa S et al. Evaluation of ventricular dysfunction using semi-automatic longitudinal strain analysis of four-chamber cine MR imaging. Int J Cardiovasc Imaging. 2015; DOI 10.1007/s10554-015-0771-2.
12) Schuster A, Morton G, Hussain ST et al. The intra-observer reproducibility of cardiovascular magnetic resonance myocardial feature tracking strain assessment is independent of field strength. Eur J Radiol. 2013; 82: 296-301.
13) Curtiss EI, Reddy PS, O'Toole JD, et al. Alterations of right ventricular systolic time intervals by chronic pressure and volume overloading. Circulation. 1976; 53: 997-1003.
14) Tantengco MV, Thomas RL, Karpawich PP. Left ventricular dysfunction after long-term right ventricular apical pacing in the young. J Am Coll Cardiol. 2001; 37: 2093-2100.
15) Nagao M, Hatakenaka M, Matsuo Y et al. Subendocardial contractile impairment in chronic ischemic myocardium: assessment by strain analysis of 3T tagged CMR. J Cardiovasc Magn Reson. 2012; 14: 14.
16) Kapetanakis S, Kearney MT, Siva A et al. Real-time three-dimensional echocardiography: a novel technique to quantify global left ventricular mechanical dyssynchrony. Circulation. 2005; 112: 992-1000.
17) Wang J, Khoury DS, Thohan V et al. Global diastolic strain rate for the assessment of left ventricular relaxation and filling pressures. Circulation. 2007; 115: 1376-1383.
18) Kuppahally SS, Akoum N, Burgon NS et al. Left atrial strain and strain rate in patients with paroxysmal and persistent atrial fibrillation: relationship to left atrial structural remodeling detected by delayed-enhancement MRI. Circ Cardiovasc Imaging. 2010; 3: 231-239.
19) Friedberg MK, Fernandes FP, Roche SL et al. Impaired right and left ventricular diastolic myocardial mechanics and filling in asymptomatic children and adolescents after repair of tetralogy of Fallot. Eur Heart J Cardiovasc Imaging. 2012; 13: 905-913.